Crack growth mechanism in some polyamides

M. J. Zhang and F. X. Zhi
Department of Materials Science and Engineering, Northwestern Polytechnical University, Xian, China
(Received 2 November 1987; revised 10 March 1988; accepted 20 May 1988)

Fracture toughness was measured with single-edge notched three-point bend specimens. The materials used were semicrystalline polymers, polyamide-66, polyamide-1010 and polyamide-610. Their fracture surface was investigated with the help of scanning electron microscopy. The crack growth mechanism is revealed and a model suggested. The stable crack growth feature of the fracture surface is the dimples. The stable crack growth includes: the crack tip blunting, the voids initiating, coalescing and extending, the fibrillated polymer rupturing and contracting, then the formation of dimples on the fracture surface. The unstable crack growth formed a fan cleavage zone. The crack growth passed along the boundaries of spherulitic crystals in which many subcracks have occurred. The mechanism of discontinuous subcrack propagation in ductile polyamide-610 was discovered. In the compressive zone of the bend specimen, the fracture mechanism is similar to the cleavage zone and exhibits shear failure response.

(Keywords: polyamide; nylon; fracture mode; crack growth mechanism; fracture toughness; *J*-integral method)

INTRODUCTION

In order to consider safety in the design of engineering components and structures, the question of a criterion for toughness in the fracture of polymeric solids has been extensively investigated from both practical and scientific viewpoints. The *J*-integral is an energy input parameter which can be used as a criterion for crack initiation in the fracture of elastic–plastic materials. Therefore, the *J*-integral method has recently received considerable attention with respect to polymeric materials[1,2]. Some problems are often encountered in ductile polymer testing, such as the energy dissipation to create plastic deformation ahead of the crack tip, the blunting effect prior to initiation and crack propagation.

Fractography, the study of the morphology of a fracture surface, is an obvious tool to elucidate the mechanism of propagation of a crack. Gaube and Kausch[3,4] studied the fractography of a high density polyethylene (HDPE) bar containing a knife cut on impact loading and bending. Chan and Williams[5] studied the phenomenon of slow stable crack growth in HDPE with scanning electron microscopy (SEM). The fracture mode of ethylene-propylene-1,4-hexadiene terpolymer (EPDM) rubber has been studied by Pal[6]. An epsilon crack tip plastic zone during discontinuous fatigue crack growth was observed in polysulphone[7] and polycarbonate[8].

This paper studies the fracture toughness of three types of polyamides using the *J*-integral method, and their fracture surface with the help of SEM. The dependence of fracture toughness on fractography is explored. Crack tip blunting, crack initiation and the crack growth mechanism are also given.

0032-3861/88/122152-07$03.00

EXPERIMENTAL

Materials and specimens

The materials used were commercial grades of polyhexamethylene hexamide (PA-66), polysebacomethylene sebacoamide (PA-1010) and polyhexamethylene sebacoamide (PA-610). The specimens were made by injection moulding. A rectangular specimen, normally $10 \times 15 \times 120$ mm, was used in the crack growth test. The Young's modulus and yield stress data were measured with dumbbell specimens. All specimens were treated

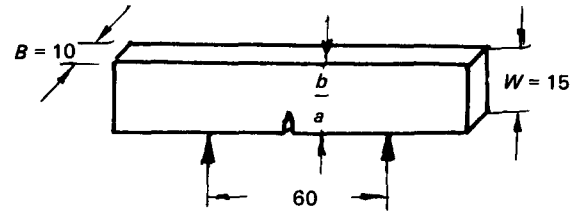

Figure 1 Single-edge notched three-point bend crack growth test specimen

Table 1 Data for the materials

Code	E (MPa)	σ_y (MPa)	ρ (g cm^{-3})	Moisture content (%)
PA-66	1300	54.6	1.12	2.5
PA-1010	950	37.8	1.05	1.5
PA-610	960	37.2	1.07	1.5

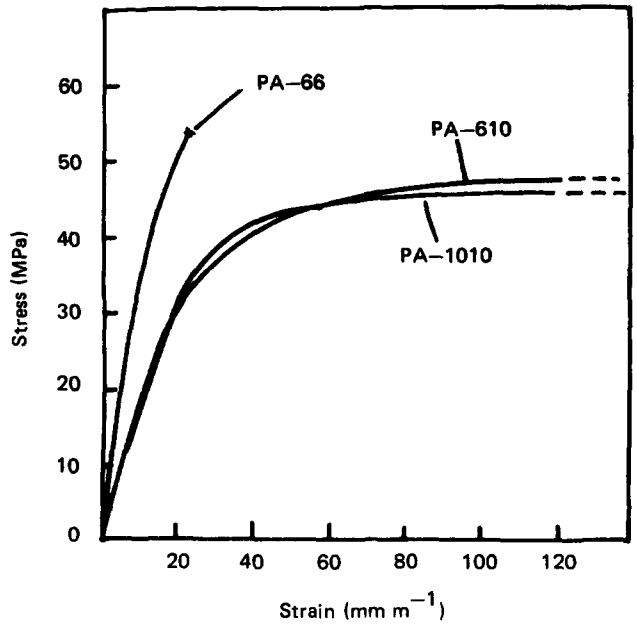

Figure 2 Stress–strain curves

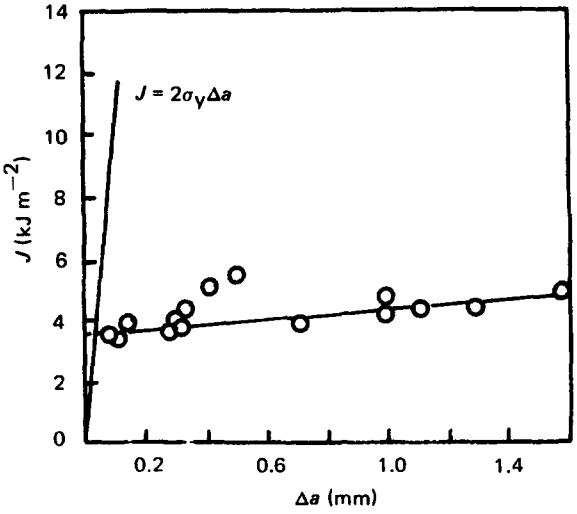

Figure 3 J–Δa data for PA-66

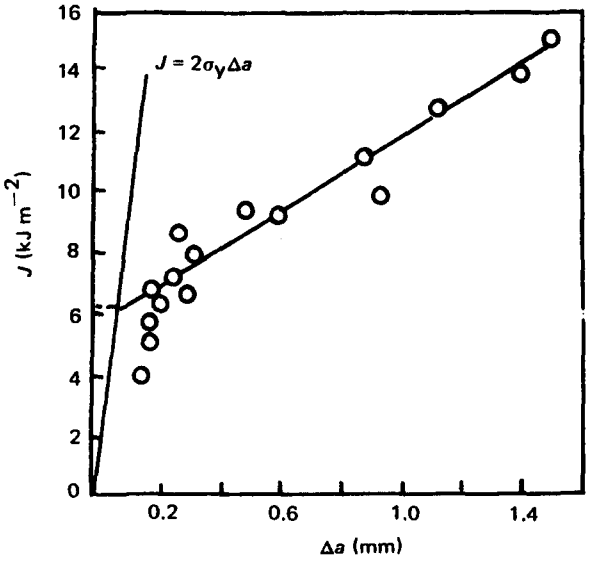

Figure 4 J–Δa data for PA-1010

with a solution of potassium acetate and water at 90–100°C for 200 h, and the treated specimens were stored at room temperature (15–25°C) and 45–70% relative humidity for more than 3 months before testing. Crack growth tests were performed with single-edge notched three-point bend specimens (*Figure 1*). The initial notches were prepared by forming 'saw-cut' slots which were then sharpened with a new razor blade. The stress–strain curves and properties of the materials are shown in *Figure 2* and *Table 1*, respectively.

The specimens, which were used for fracture mechanism observation, were tested as above, but no dye was injected during the testing. In order to confirm the crack tip blunting and crack propagation mechanism, the smaller specimens with a cross-section of 4 × 5 mm were cut, and a V-type notch was created and then sharpened with a new razor blade. The small specimen, which was subjected to a constant bend strain by a fixture, was observed using SEM.

The fracture surface was gold sputtered and examined in an Amray 1000B SEM.

Fracture toughness test

Fracture toughness tests were carried out in a universal testing machine at a bending rate of 1 mm min^{-1} at room temperature (23–25°C) and the three-point bend rig had a span of 60 mm. The loadline displacement was measured from the amount of machine cross-head motion, and the area under the load–displacement curve was obtained with an area integrator. A series of identical specimens were loaded to different values of load-point displacement to obtain different J-values and then unloaded. The crack growth was marked by dyeing during testing. A permeable dye was injected into the specimen notch. The specimens tested were bent to failure after the dye drying. The amount of crack growth, Δa, and ligament, b were measured by a microscope (× 50) interval to an accuracy of ± 0.01 mm.

J-integral method

The J-integral method, which is a multiple specimen resistance curve method, was developed by Landes *et*

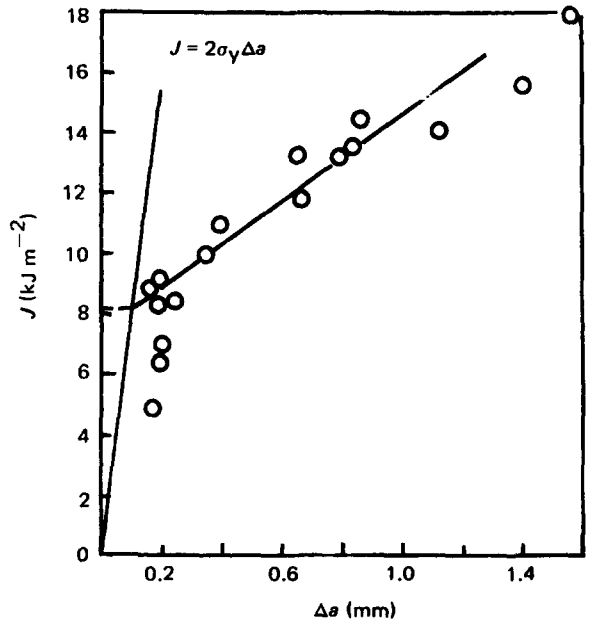

Figure 5 J–Δa data for PA-610

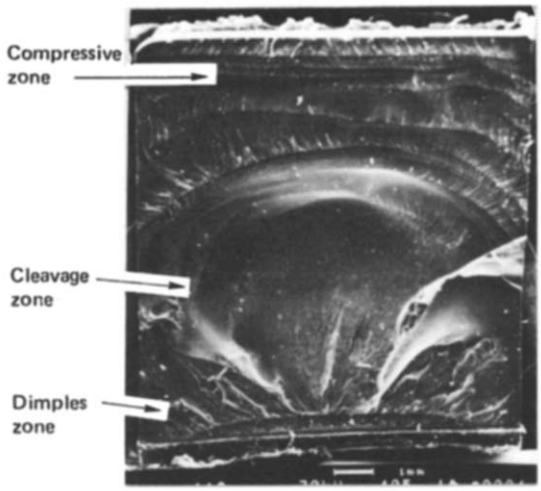

Figure 6 Fracture surface of PA-66

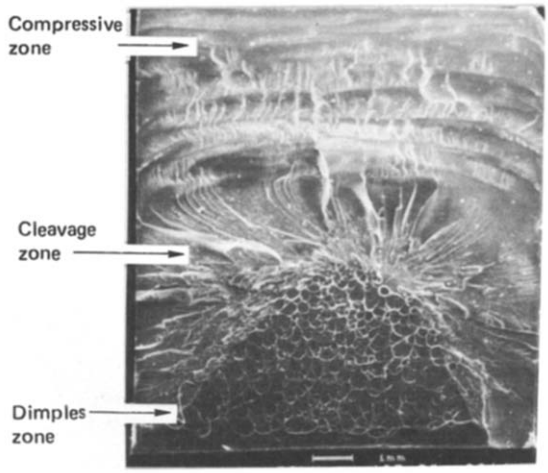

Figure 7 Fracture surface of PA-1010

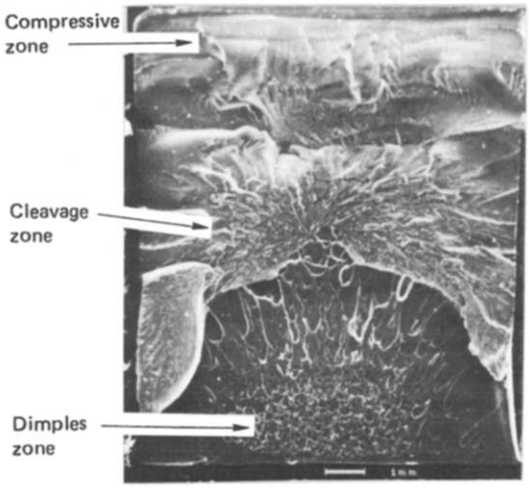

Figure 8 Fracture surface of PA-610

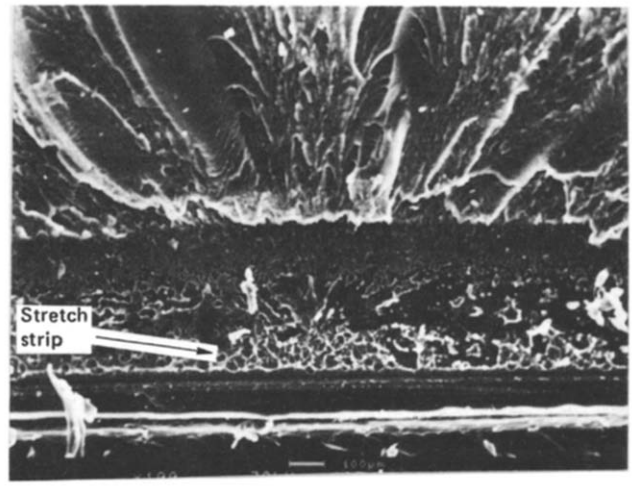

Figure 9 Higher magnification of the stretch strip and the dimples zone in *Figure 6*

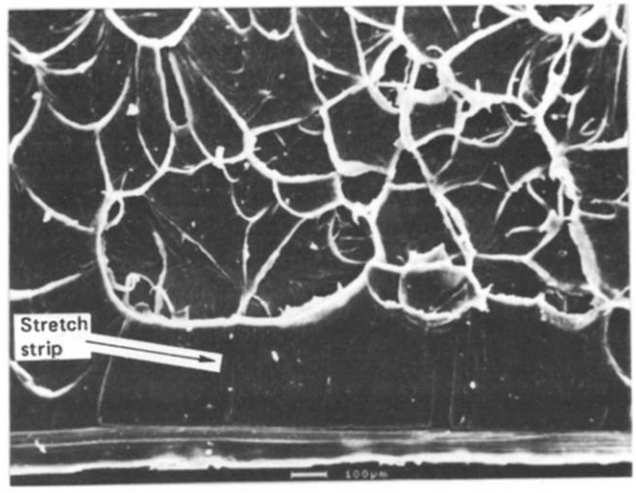

Figure 10 Higher magnification of the stretch strip and the dimples zone in *Figure 7*

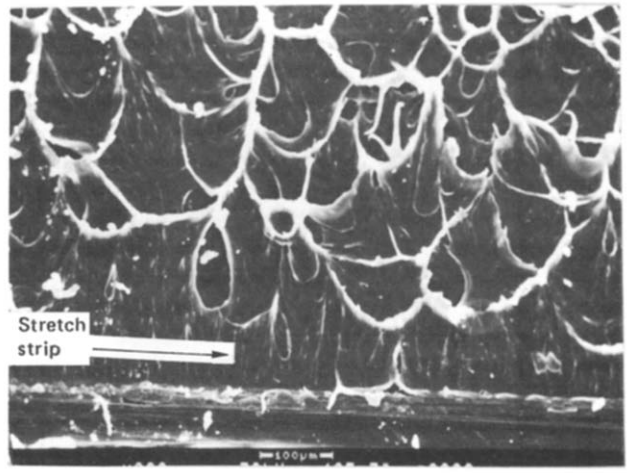

Figure 11 Higher magnification of the dimples zone and the stretch strip in *Figure 8*

al.[9] This method consists of loading a series of specimens of identical dimensions and determining the energy (U) associated with different values of load-point displacement. For a three-point bend-type specimen with a span-to-depth ratio of 4, the J-integral value is approximately given by

$$J = 2U/Bb \quad (1)$$

where U is the area under load *versus* load-point displacement curve, B is the specimen thickness and b is the ligament length.

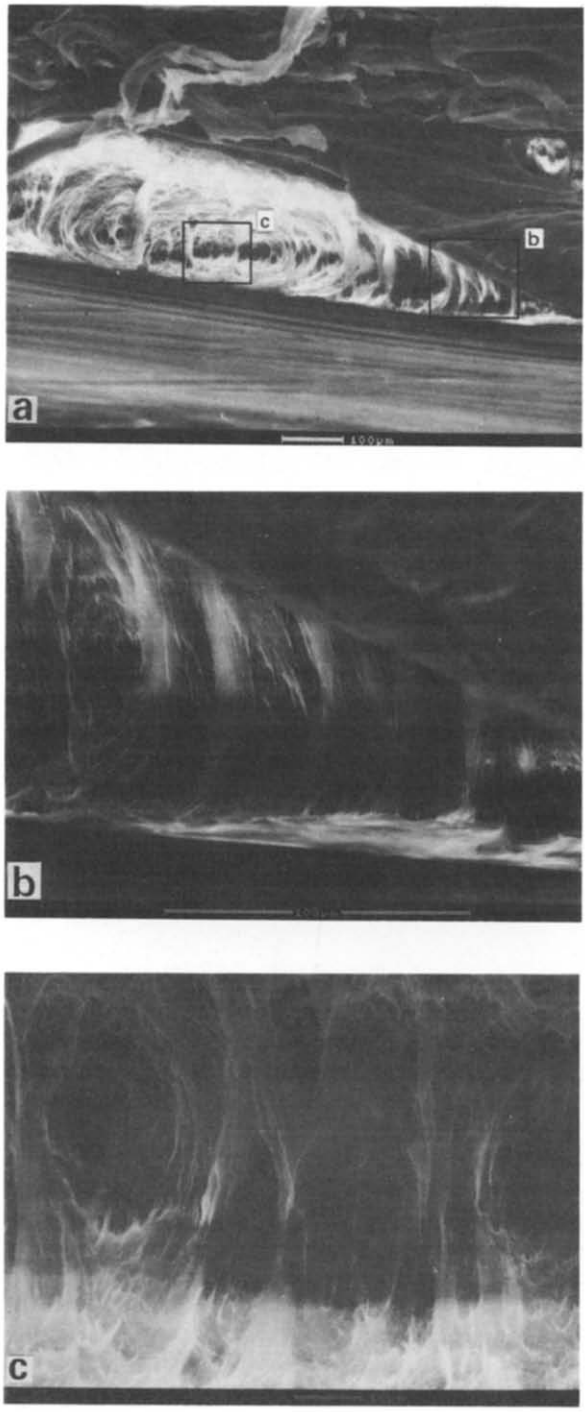

Figure 12 Crack tip blunting and crack initiating views at crack opening direction. (b) is higher magnification of right local of crack tip in (a), and (c) is higher magnification of centre local of crack tip in (a)

A critical value of J is defined as the energy release rate when a stable crack begins to grow. For elastic-plastic conditions, the crack tip blunting occurs forming a crack-opening stretch zone prior to actual crack growth. When a blunted crack is assumed to be a semi-circular profile, the crack tip movement due to blunting is given by

$$J = 2\sigma_y \Delta a \tag{2}$$

where σ_y is the uniaxial yield stress and Δa is the apparent crack growth. The J-value at the onset of actual growth is determined by the intersection of the blunting line, calculated by equation (2), and the line plotting the J-value against actual crack growth.

Under the plane strain conditions, the specimen size criteria suggested by ASTM Method E813-81 are expressed in terms of the J-value:

$$B, (W-a) \geqslant 25(J_{Ic}/\sigma_y) \tag{3}$$

The results show that the specimen size meets the above criteria. The J_{1c} value determined may be considered to be valid.

RESULTS AND DISCUSSION

Fracture toughness

The J-values at the point of unloading are plotted as a function of crack growth (*Figures 3–5*). These data may be considered to be within experimental error because the multiple specimen method exhibits greater scatter. The crack resistance curve is obtained, from which a critical value of J for crack initiation can be determined. The critical J values for PA-66, PA-1010 and PA-610 are 3.2, 6.3 and 8.1 kJ m^{-2}, respectively. The resistance of the materials to stable crack extension should be expressed by the slope of the resistance curve or $dJ/d\Delta a$, and are 1.1, 6.2 and 7.0 MPa for PA-66, PA-1010 and PA-610, respectively.

It should be noted that no experimental data are on the blunting line, although we attempted a smaller crack

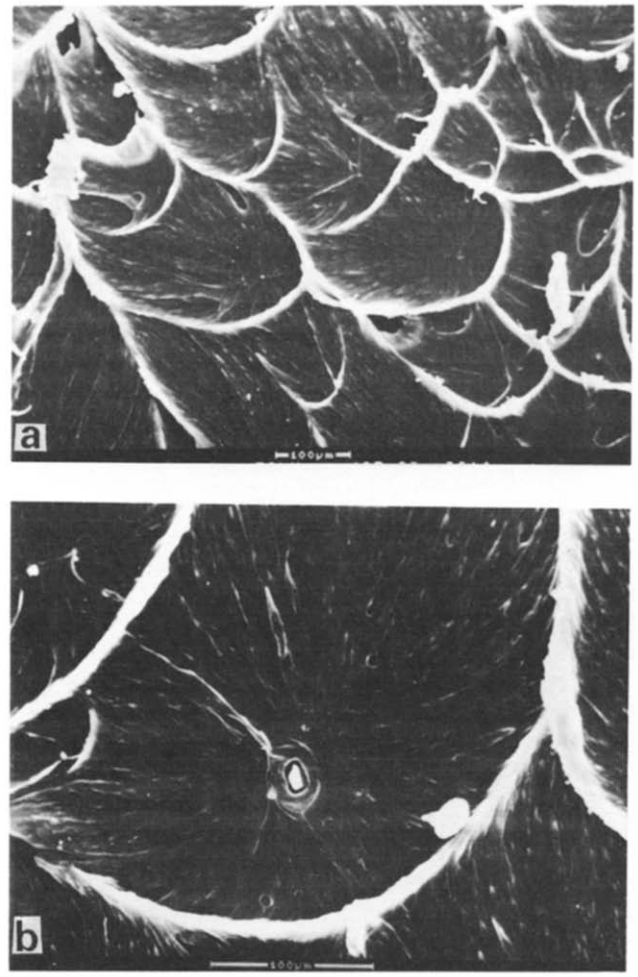

Figure 13 Higher magnification of dimple zone for PA-1010 in *Figure 10*. (b) is higher magnification of (a)

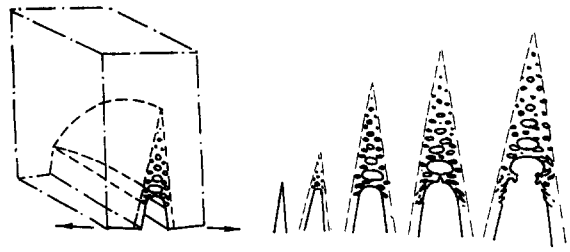

Figure 14 Diagram showng crack initiation and growth

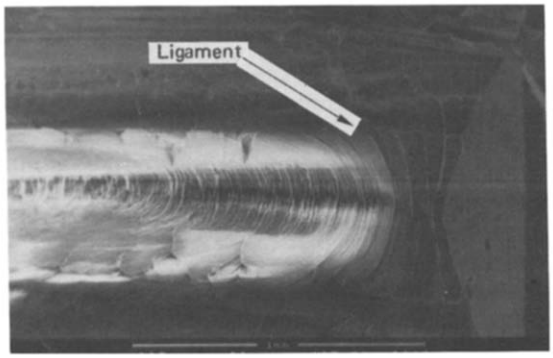

Figure 15 Ligament at edge of specimen

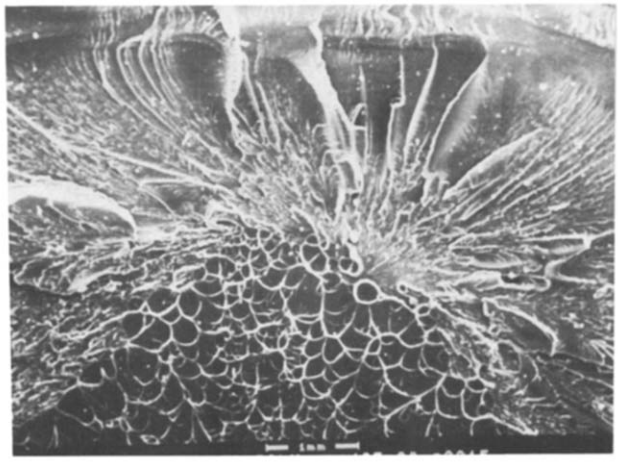

Figure 16 Fractography of cleavage zone for PA-1010

extension. Narisawa[2] reported a similar phenomenon. One of the reasons may be that some dye permeated into the blunting crack tip. Another reason may be that the blunting line does not express the complexity of actual crack tip blunting.

Therefore, it is necessary to further study crack tip blunting and the fracture surface as important information and possible clues about the fracture mechanism may be obtained.

Crack growth mechanism

It was found from fracture surface studies that the fractography for the three types of polyamide are similar as shown in *Figures 6–8*. They are all divided into three distinct zones:

a thumbnail-type zone of crack initiation and stable crack propagation from an initial notch, or stretch strip and dimple zone;

a zone of unstable or rapid crack propagation, or cleavage fracture zone;

a compressive zone of bending specimen, where there is a new zone of unstable crack propagation.

The size of the stretch strip and dimples zone exhibits obvious differences for the three types of polyamide. Higher magnification of these zones is shown in *Figures 9–11*, respectively. The dimples zone is the biggest for PA-610 and the smallest for PA-66. The area of this zone may depend on the fracture toughness of the material.

In order to reveal the crack tip blunting and onset of the crack, the small specimen with the V-type notch which

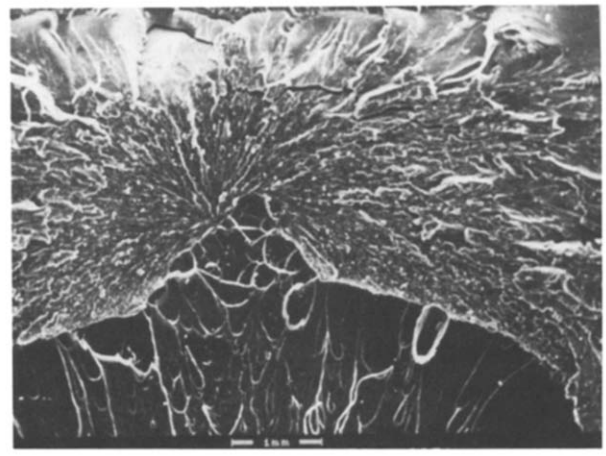

Figure 17 Fractography of cleavage zone for PA-610

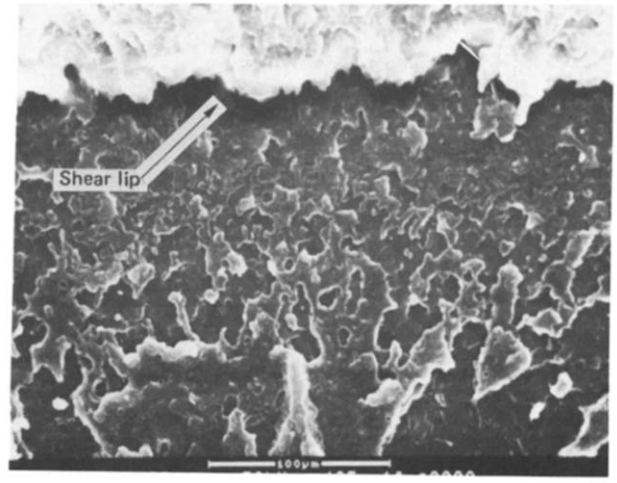

Figure 18 Shear lips of cleavage zone for PA-66

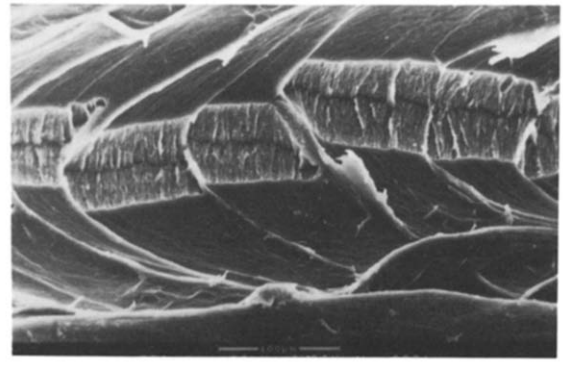

Figure 19 Local crack propagation and striations (at crack opening)

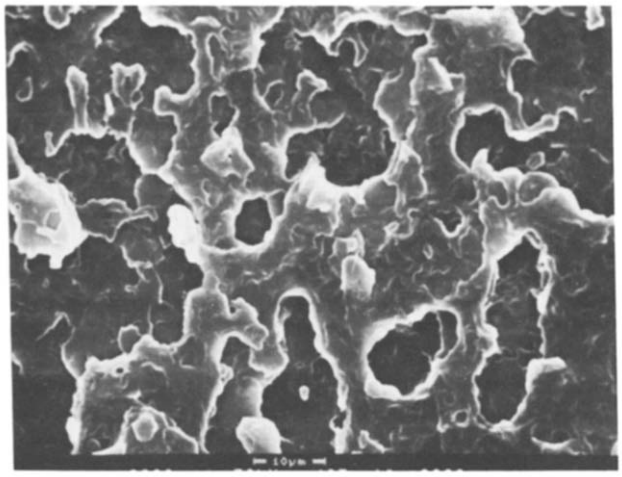

Figure 20 High magnification of cleavage zone for PA-66

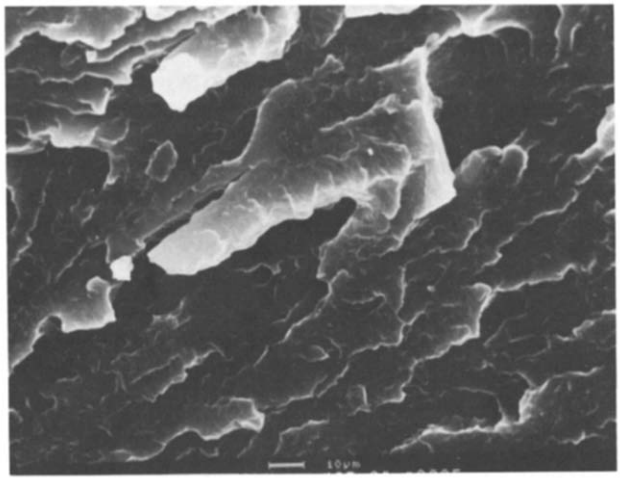

Figure 21 High magnification of cleavage zone for PA-1010

was subjected to a constant bend strain, was observed using SEM. The crack tip blunting and initiating is shown in *Figure 12*. At the centre, the crack is just beginning to grow, and at the side, the initial notch is only in the blunting stage. *Figure 12b* shows the crack blunting feature which consists of a uniform fibril structure interspersed with voids. *Figure 12c* shows the crack initiating feature, bigger voids are surrounded by a fibril structure which is interspersed with microvoids, and some ruptured fibril structure.

The edge of the three-point bend specimen is in the plane-stress state and the centre of the specimen is in the plane-strain state. As the initial notch tip is opening, the free surface of the tip is not under triaxial stresses. Therefore, orientation is possible so that the spherulitic crystalline structure becomes a fibrillated structure which causes greater deformation and constrains the crack to propagate into the sample with a widening crack front. The fibrillated structure at the initial notch front ruptured and contracted to form a stretch strip on the fracture surface.

The centre ahead of the crack tip is under triaxial stresses. The microvoids are created by the many internal defects and impurities. With increasing stress, the voids are extended and coalesced, or the new voids are initiated. The growing free surfaces of rounded voids are also not under triaxial stresses. The walls of voids can also be oriented to form a fibrillated structure and part of the energy is absorbed and spread over a larger area. The fibril structure of the void walls was ruptured and contracted to form the dimples.

Figure 13 shows that there is an initial source for many dimples, and the markings indicate that some smaller voids were coalesced, and the void wall was extended.

It may be noted from *Figure 12* that there is a deformation band on the two sides of the main crack, and its thickness depends on the ductility of the material.

A possible mechanism for crack tip blunting, crack initiation and growth are shown in *Figure 14*.

It should be noted that greater deformation can occur at the edge of the specimen near the crack tip because it is in the plane-stress state. *Figure 15* shows clearly that the crack has extended (but the ligament at specimen edge does not rupture) where the material was highly stretched and constricted transversely so that the specimen surface caved in.

The ligament at the specimen edge is in a load carrying capacity, which is one of the reasons why the crack can stably propagate.

With the crack growing and the edge of the specimen tearing, the stress of the crack front increases sharply. Orientation becomes impossible so that characteristics of

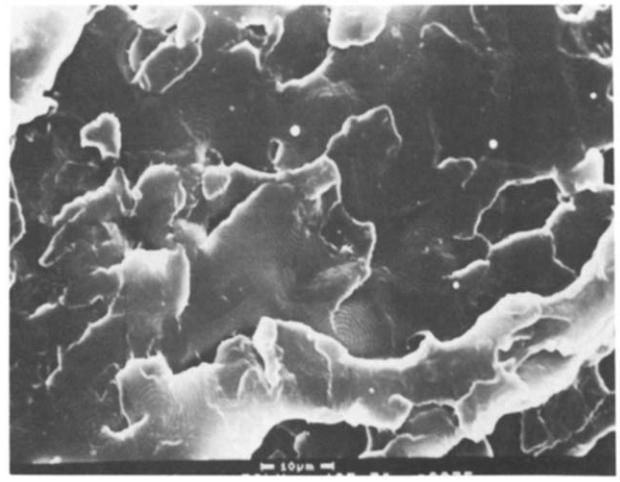

Figure 22 High magnification of cleavage zone for PA-610

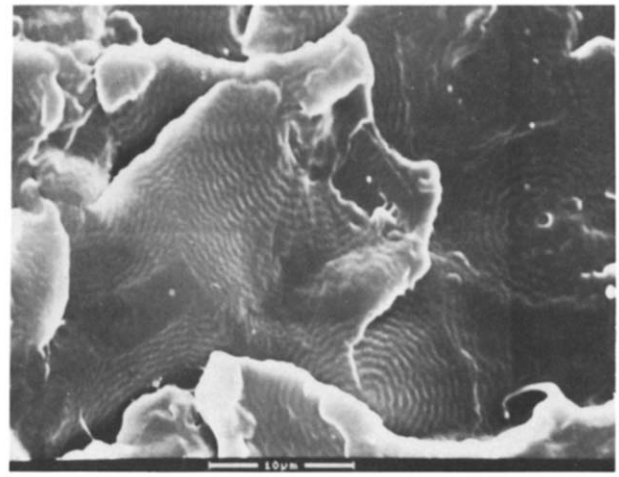

Figure 23 Higher magnification of *Figure 22*

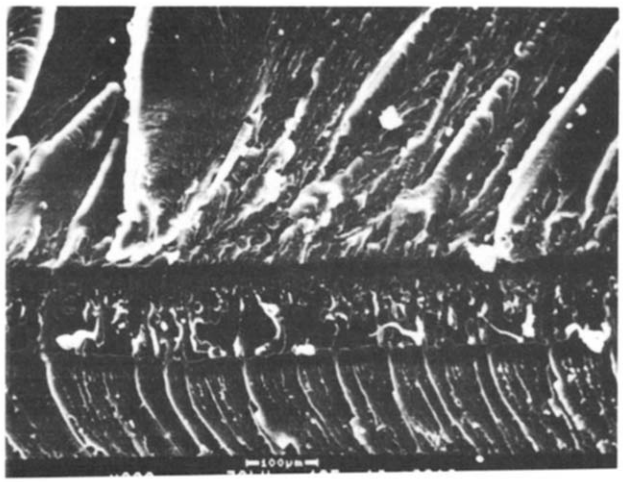

Figure 24 Fractography of compressive zone for PA-66

usual brittle failure are exhibited. The cleavage zone where the crack propagates rapidly was formed as shown in *Figures 9, 16* and *17*. The crack initiation is at the centre and the crack front follows one of the $\pm 45°$ shear zone boundaries, forming the well-known 45° shear lips on the fracture surface, as shown in *Figure 18*. The shear lips are not clear for ductile PA-1010 and PA-610.

Another characteristic of cleavage is the striations fanning out. The striations result from the subcrack ahead of the main crack not being in the plane.

Figure 19 shows the path of local crack propagation ahead of the main crack, and the striations which were formed between the two distinct crack planes. Although the crack growth condition is different from that of the cleavage zone, the principle of forming striations is consistent.

The third characteristic of cleavage is that the crack passes along the boundaries of the spherulitic crystalline phase. Ahead of the cleavage crack occur many subcracks between the spherulitic crystalline phase, in which there are more defects, and the ends of the chain. When a propagating crack passes from a grain having a subcrack into another grain having a different subcrack, the crack must propagate through the second grain in the new plane. Therefore, several planes are shown on the cleavage fracture surface. *Figures 20* and *21* show several cleavage planes and the spherulitic crystalline feature which has a diameter of 3–8 μm for PA-66 and PA-1010. Because PA-66 has less fracture toughness, the rupture at the spherulitic crystalline boundaries is quite clear. Although the spherulitic feature of PA-610 is not clear, several cleavage planes are similar to PA-66 and PA-1010 as shown in *Figure 22*. Interestingly, the shell striation in the facets can be seen obviously (*Figure 23*). This is a strong indication for the mechanism of discontinuous subcrack propagation. Because of the spherulitic crystalline imperfection, the secondary crack propagation is constrained. The shell markings on the fracture facet show that the subcrack propagation has had a history of blunting, propagation, reblunting and repropagation for PA-610. It shows that PA-610 is very capable of the resistance to crack.

For the compressive zone of the bending specimen, the fracture surface topography is shown in *Figure 24*. There are several shear layers and the 45° shear lips on the fracture surface in every layer can be seen clearly. This is an indication that shear stress dominates in compression.

CONCLUSIONS

The *J*-integral method for three-point bend specimens using dyeing for marking crack growth is available for polymeric materials. For semicrystalline polymers, the spherulitic structure ahead of the crack tip can be elongated to form an oriented fibrillated structure with many voids, which can be extended.

The voids form from triaxial stresses, but the initial source of voids is defects and impurities. With the voids forming, the void walls are not under triaxial stresses, which is favourable for orientation and fibrillation. Therefore, the dimples are the fracture characteristics of stable crack growth.

During the rapid crack propagation, the main crack propagates too fast to elongate the spherulitic structure so that the crack extends along the interface of the spherulitic crystalline phase. Many subcracks occur ahead of the main crack at the interface of the spherulitic crystalline phase.

Subcrack propagation is discontinuous for highly ductile polymeric materials.

REFERENCES

1 Hashemi, S. and Williams, J. G. *Polym. Eng. Sci.* 1986, **26**, 760
2 Narisawa, I. *Polym. Eng. Sci.* 1987, **27**, 41
3 Gaube, E. and Kausch, H. H. *Int. Cont. Fract. Munich*, 1973, I PI V1-311
4 Gaube, E. and Kausch, H. H. *Kunststoffe* 1973, **63** (6), 391
5 Chan, M. K. V. and Williams, J. G. *Polymer* 1983, **24**, 234
6 Pal, P. K. and De, S. K. *Polymer* 1984, **25**, 855
7 Matsumoto, D. S. and Takemori, M. T. *Polym. Commun.* 1983, **24**, 41
8 Takemori, M. T. *Polym. Eng. Sci.* 1982, **22**, 937
9 Landes, J. D. and Begley, J. A. *ASTM STP* 632, **1977**, 57